Inhibition of phosphoinositide-3 kinases γ/δ ameliorates pulmonary granuloma by rescuing Treg function in a sarcoidosis model

XIAN ZHANG[1*], QIANQIAN DAI[1*], JIAJIA SHAN[1], SHIYUN ZHANG[1], BIN ZHANG[1], SIYANG LIU[1], YIXUE ZHANG[1], YING WANG[1], XIAOJIE LI[1], XUGUANG JIN[1], DONGMEI LIANG[1], JINGJING DING[2], YONG WANG[3] and YANTING WEN[1]

[1]State Key Laboratory of Pharmaceutical Biotechnology and Jiangsu Key Laboratory of Molecular Medicine, The Affiliated Nanjing Drum Tower Hospital, Medical School of Nanjing University, Nanjing, Jiangsu 210093; [2]Department of Respiratory Medicine and Jiangsu Key Laboratory of Molecular Medicine, The Affiliated Drum Tower Hospital of Nanjing University Medical School, Nanjing, Jiangsu 210003; [3]State Key Laboratory of Analytical Chemistry for Life Science and Jiangsu Key Laboratory of Molecular Medicine, The Affiliated Nanjing Drum Tower Hospital, Medical School of Nanjing University, Nanjing, Jiangsu 210093, P.R. China

Received October 10, 2022; Accepted February 17, 2023

DOI: 10.3892/etm.2023.11923

Abstract. Sarcoidosis is a multisystem inflammatory disease characterized by the development of Th1/Th17/regulatory T cells (Tregs)-related non-caseating granulomas. Phosphoinositide-3 kinases δ/γ (PI3Kδ/γ) play an important role in the maintenance of effective immunity, especially for Tregs homeostasis and stability. In the present study, superoxide dismutase A (SodA) stimulation was used to establish the sarcoidosis mouse model. The second immune stimulus was accompanied by CAL-101 (PI3Kδ inhibitor) or AS-605240 (PI3Kδ/γ inhibitor) treatment. To detect the effect of the PI3Kδ/γ inhibitor on the morphology of pulmonary granuloma and the activation of the PI3K signaling pathway, hematoxylin and eosin staining and immunofluorescence and western blotting was used, respectively. Fluorescence-activated cell sorting analysis and reverse transcription-quantitative PCR were adopted to detect the effect of the PI3Kδ/γ inhibitor on the SodA-induced sarcoidosis mouse model in respect to immune cell disorder and the function of Treg cells, with $CD4^+CD25^-$ T cells and $CD4^+CD25^+$ T cells sorted by magnetic cell sorting. The results demonstrated that the inhibition of PI3Kδ/γ by transtracheal CAL-101/AS-605240 administration facilitated pulmonary granuloma formation. These therapeutic effects were associated with certain mechanisms, including suppressing the aberrantly activated PI3K/Akt signaling in both pulmonary granuloma and Tregs, particularly rescuing the suppressive function of Tregs. Notably, CAL-101 was more effective in immune modulation compared with AS-605240 and could overcome the aberrantly activated Akt in the lung and Tregs. These results suggest that PI3K/Akt signaling, especially the PI3Kδ subunit, can play a key role in optimal Tregs-mediated protection against pulmonary sarcoidosis. Therefore, transtracheal usage of PI3Kδ/γ inhibitors is an attractive therapy that may be developed into a new immune-therapeutic principle for sarcoidosis in the future.

Correspondence to: Dr Yanting Wen, State Key Laboratory of Pharmaceutical Biotechnology and Jiangsu Key Laboratory of Molecular Medicine, The Affiliated Nanjing Drum Tower Hospital, Medical School of Nanjing University, 22 Hankou Road, Nanjing, Jiangsu 210093, P.R. China.
E-mail: wenyanting@nju.edu.cn

Professor Yong Wang, State Key Laboratory of Analytical Chemistry for Life Science and Jiangsu Key Laboratory of Molecular Medicine, The Affiliated Nanjing Drum Tower Hospital, Medical School of Nanjing University, 22 Hankou Road, Nanjing, Jiangsu 210093, P.R. China
E-mail: yongwang@nju.edu.cn

*Contributed equally

Key words: sarcoidosis, PI3K/Akt signaling, regulatory T cell, CAL-101, AS-605240

Introduction

Sarcoidosis is a chronic inflammatory disease characterized by granuloma formation and a gradual loss of lung function (1). Sarcoidosis can affect any organ, but most commonly, it affects the lungs and the intrathoracic lymph nodes (2). The granuloma is distinguished by a core of epithelioid histiocytes and multinucleate giant cells, interspersed by $CD4^+$ T lymphocytes with a Th1 immuno-phenotype, as well as a minority of $CD8^+$ T lymphocytes, fibroblasts and B lymphocytes (3-5). It is difficult to tailor treatment to specific disease phenotypes or disease mechanisms. Thus, at present, the treatment relies primarily on immunosuppression with steroids and/or

steroid-sparing drugs to palliate symptoms, switch off acute inflammation and prevent end-organ disease (6).

Regulatory T cells (Tregs)/Th17 and Th1/Th2 paradigms play a role in the pathogenesis of sarcoidosis (7,8). The population of Tregs act as the key controllers for limiting immunopathology and maintaining immune homeostasis (9). The lymph nodes and granulomas of sarcoidosis patients are flooded with Treg cells (10), whereas their presence in blood demonstrates conflicting results. Even by the same team of researchers, patients with sarcoidosis have been reported to have various amounts of Tregs, which are sorted into higher, lower and normal groups (9,11). These controversial numbers of Tregs may be associated with the stage of the disease. Patients with active sarcoidosis have increased numbers of Tregs, while patients with inactive sarcoidosis and spontaneous remission have normal or decreased numbers of Tregs (3,12-15). Our previous superoxide dismutase A (SodA)-induced sarcoidosis models showed changes in Treg numbers correlated with disease phases (16,17). This demonstrates that, compared with the function of Tregs in healthy individuals, the function of Tregs in patients with sarcoidosis is severely impaired (3). Due to this impairment, Tregs fail to inhibit the persistent and excessive inflammatory responses of sarcotic lesions and immune homeostasis cannot be maintained (9). In addition, without the ability to actively regulate reactive T cells, Tregs can only partially inhibit early granuloma formation and have no positive effects on the formed granulomatous lesions (12).

In our previous study, patients and mice with sarcoidosis both showed phosphoinositide 3-kinase (PI3K)/Akt signaling pathway activation, affecting FoxP3 expression in Tregs (14,16,17). It has been reported that controlling PI3K signaling in Tregs is critical for maintaining their homeostasis, function and stability (18). Previously, we reported that inhibition of PI3K/Akt signaling by BKM120 (an inhibitor of pan-class I PI3K) or LY294002 (an inhibitor of PI3Kα, δ and β) reverses the disturbance of Th1/Th17/Tregs and improves the function of Tregs in SodA-induced sarcoidosis. Notably, BKM120 is more effective compared with LY294002 in restoring the immunosuppressive function of Tregs, which demonstrates that PI3K/Akt signaling in Tregs may be associated with the PI3Kp110γ subunit in SodA-induced sarcoidosis (17). Thus, understanding its intrinsic effects in Sarcoidosis is necessary to formulate future therapies that favor homeostasis of Tregs in the disease. Therefore, the present study examined the impact of the effects of PI3Kp110γ/δ inhibition on the function of Tregs in SodA-induced sarcoidosis, especially at the chosen time point when the number of Tregs is normal.

Materials and methods

Animals. First, six-week-old female C57BL/6J mice (n=30) weighing 20-25 g were purchased from the Shanghai Lab. Animal, Research Center. Mice were maintained under a specific pathogen-free environment (temperature, 22±1˚C; relative humidity, 50±5%; and 12-h light/dark cycle). Water and food were supplied *ad libitum*. All *in vivo* manipulations were performed under protocols approved by the Institutional Animal Care and Use Committee of Nanjing University Medical School (approval no. SCXK-Jiangsu-2019-0056). Mice were acclimated for at least one week before use. Mice were euthanized using cervical dislocation following carbon dioxide inhalation according to according to the American Veterinary Medical Association guidelines (19). Euthanasia was performed in a dedicated box with CO_2, using a gradual 30% vol/min displacement rate. The percentage of CO_2 and O_2 used was 6:4. Based on the humane end point criteria, the distress of the animals was constantly monitored. The condition of the mice were checked daily. Mice were sacrificed when they developed hypothermia, inability to stand and wounds that did not heal. None of the mice developed symptoms requiring sacrifice during the experiment.

SodA-induced sarcoidosis model. Sarcoidosis was induced based on a method provided by Swaisgood *et al* (20). In brief, on the first day, mice were pretreated with 20 mg of mycobacterial SodA peptide (Ala-Ala-Ala-IIe-Ala-Gly-Ala-Phe-Gly-Ser-PheAsp-Lys-Phe-Arg; GenBank accession no. DQ768096) dissolved in 0.25 ml of incomplete Freund's adjuvant (MilliporeSigma) by subcutaneous injection. Subsequently, 14 days later, the SodA-sensitized mice were challenged with 6000 N-hydroxysuccinimide-activated Sepharose 4B naked beads [in 0.5 ml of phosphate-buffered saline (PBS)] covalently coupled to SodA by tail vein injection. After 28 days, lung tissues were collected to establish sarcoidosis.

CAL-101/AS-605240 treatment. SodA-induced sarcoidosis mice were randomly divided into five groups the day after tail vein injection. A total of 2 mg/kg of CAL-101 (PI3Kδ inhibitor; TargetMol Chemicals, Inc.) or AS-605240 (PI3Kγ inhibitor; TargetMol Chemicals, Inc.) were respectively given to the mice via airway on days 15, 16, 29, 30, 36 and 37 (Fig. 1A). DMSO was applied to group sarcoidosis. As the positive control group, dexamethasone was administered to mice by intraperitoneal injection at 5 mg/kg. The other healthy mice were kept as the control group.

Histopathology and immunofluorescence. Right upper lung tissues were fixed in 4% paraformaldehyde at 4˚C overnight, dehydrated and cut into 4-μm thick sections after being embedded in paraffin. Tissue sections were routinely stained with hematoxylin and eosin (H&E) for conventional morphological evaluation under the light microscope (Olympus Corporation). The specific methods were as follows: First, the sections were placed in an oven and heated at 60˚C for 1 h. The following steps are all performed at room temperature; the paraffin sections were immersed in xylene solution for 10 min, and then immersed in a new xylene solution for another 10 min; Then the tissue sections were immersed in 100, 95, 90, 80, 75, and 50% alcohol solution for 2 min, respectively. Finally, the tissue sections were immersed in ddH_2O for 5 min. The sections were placed in hematoxylin and stained for 15 min. After staining, the sections were washed with ddH_2O for 5 min to turn blue. Then the sections were placed in 1% hydrochloric acid ethanol solution for about 5 sec, as soon as the sections turned red, they were placed in ddH_2O to restore the blue color. After this, the rinsed sections were soaked in 50, 70 and 80% alcohol for 3 min in turn, and then counterstained in 0.5% eosin ethanol solution for 1-3 min. The excess red color was washed off with 95% alcohol, and the sections soaked in

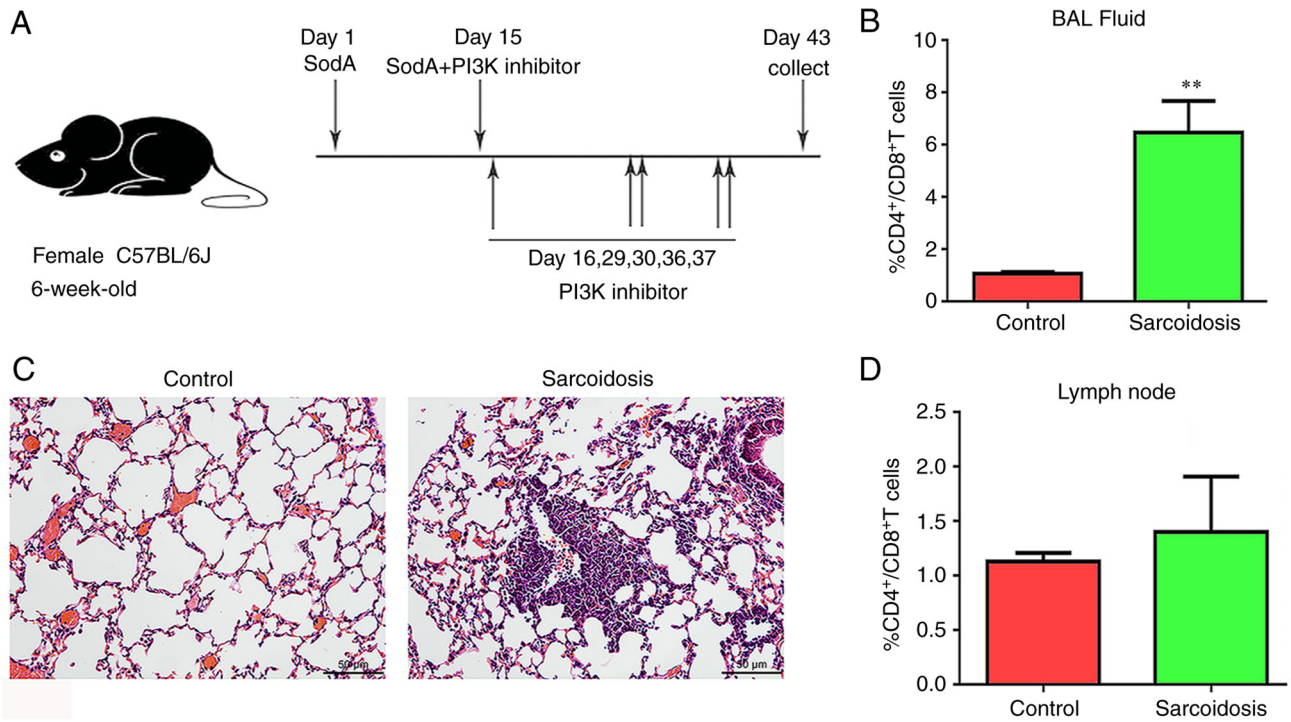

Figure 1. Histomorphometrical analysis and cytologic examination of SodA-induced sarcoidosis. (A) Modeling diagram and PI3K inhibitors interventions. (C) Hematoxylin and eosin staining of the lung. Magnification, x100. The ratios of $CD4^+/CD8^+$ T cells in (B) BALF and (D) lymph nodes were tested using flow cytometry (n=6). $^{**}P<0.01$. SodA, superoxidase A; BALF, bronchoalveolar lavage fluid.

100% alcohol for 5 min, then the excess ethanol washed off with ddH_2O, and the sections soaked in xylene for 5 min, and new xylene replaced for another 5 min. Finally the neutral gum was diluted with xylene to the appropriate viscosity and the slide sealed.

Immunofluorescence was performed by using p-PI3K p85 antibody (cat. no. 4228S; Cell Signaling Technology, Inc.), p-Akt (ser473) rabbit monoclonal antibody (cat. no. 4060; Cell Signaling Technology, Inc.), Alexa Fluor 488 goat anti-rabbit IgG (cat. no. FMS-MSAF48801; Nanjing Fcmacs Biotechnology Co., Ltd.) and Alexa Fluor 647 goat anti-mouse IgG (cat. no. FMS-RBAF64701; Nanjing Fcmacs Biotechnology Co., Ltd.). The dilution ratio of all primary antibodies was 1:500 and the dilution ratio of secondary antibodies was 1:1,000. The specific method was as follows: The prepared paraffin sections of lung tissue are placed on a shelf and heated in a 60˚C oven for 30 min. Tissue sections were soaked in xylene for 20 min and then soaked in 100, 95, 90, 80, 75 and 50% alcohol solutions for 3 min, respectively. The sections were soaked in ddH2O for 5 min, then re-soaked after changing the water and repeated three times. 0.5% TritonX-100 was prepared with PBS, preheated in advance, and added into the tissue section for 10 min, so that the antibody could fully enter the cell for reaction. The antigen repair solution was heated in the microwave oven until it boiled slightly and the sections were put into the heated antigen repair solution. The microwave oven was turned to medium heat for 2 min, then to medium heat for 2 min, then to medium heat for 7 min. After the heating stopped, the antigen recovery solution was returned to room temperature. The sections are placed flat on a shelf in a box of water to keep the culture moist and prevent the sections from drying out. Then, ~200 μl of blocking solution (PBS containing 5% BSA) was dropped on and around the tissue surface and incubated at room temperature for 1 h. Then, 100 μl diluted primary antibody solution was added and incubated at 4˚C overnight. Dilute fluorescent secondary antibody (100 μl) was added and incubated at room temperature and dark for 1.5 h. DAPI was diluted with PBS at a dilution ratio of 1:1,500 and 100 μl was added to each section and incubated at room temperature and away from light for 10-15 min. Finally, the sections were sealed with anti-fluorescence quencher. Fluorescence images were obtained using confocal microscopy (cat. no. FV3000; Olympus Corporation). All analysis was performed by a pathologist who was independent of this study, blindly.

Western blotting. The total protein from lung tissues was collected using chilled RIPA lysis buffer (Beyotime Institute of Biotechnology), and protein concentration was measured according to the BCA kit (Takara, Bio, Inc.) instruction method. Equal lysates (50 μg) were resolved on 10% SDS-PAGE and transferred to PVDF membranes with transfer buffer (25 mM Tris-base, 0.2 M Glycine, 20% Methanol, pH 8.5). Membranes were blocked in 5% bovine serum albumin (BSA) for 2 h at room temperature and then subjected to primary antibodies against PI3 Kinase p85α (6G10) mouse monoclonal antibody (cat. no. 13666; Cell Signaling Technology, Inc.), Human/Mouse/Rat Akt pan specific antibody (cat. no. 4691; Cell Signaling Technology, Inc.), p-PI3 Kinase p85 antibody (cat. no. 4228S; Cell Signaling Technology, Inc.), p-Akt (ser473) rabbit monoclonal antibody (cat. no. 4060; Cell Signaling Technology, Inc.) and GAPDH Human/Mouse/Rat polyclonal antibody (cat. no. BS65529, Bioworld Technology). Membranes were incubated overnight at 4˚C with primary

antibodies. The membranes were then incubated with HRP-labeled goat anti-rabbit IgG(H+L) (A0208, Beyotime Institute of Biotechnology) or HRP-labeled goat anti-mouse IgG(H+L) (A0216, Beyotime Institute of Biotechnology) for 2 h at room temperature, depending on the species. All primary and secondary antibodies were diluted 1:1,000. For visualization, chemiluminescence was performed with ECL Western Blotting Substrate (Tanon Science and Technology Co., Ltd.). Quantification of western blots was performed with Image J (ImageJ 1.49; National Institutes of Health).

Fluorescence-activated cell sorting analysis (FACS). To obtain bronchoalveolar lavage fluid (BALF), the lungs were flushed via the trachea using 1 ml PBS. BALF was recollected, and cells were stained using 0.25 μl fluorescein isothiocyanate-conjugated anti-mouse CD4 (Miltenyi Biotec GmbH) and 0.625 μl APC conjugated anti-mouse CD8a (eBioscience; Thermo Fisher Scientific, Inc.). The antibody was added and incubated for 0.5 h. Mononuclear cells (MNCs) were obtained by grinding the mediastinal lymph nodes and then suspending them in RPMI 1640 (Thermo Fisher Scientific, Inc.). For MNCs staining, the following antibodies were used: FITC CD4 monoclonal antibody (cat. no. GK1.5), PE CD8a monoclonal antibody, APC CD25 monoclonal antibody (cat. no. PC61.5), APC IFNγ monoclonal antibody (cat. no. XMG1.2), PE IL-4 monoclonal antibody (cat. no. 11B11), PE FoxP3 monoclonal antibody (cat. no. FJK-16s) and PE IL-17A monoclonal antibody (cat. no. eBio17B7; all from eBioscience; Thermo Fisher Scientific, Inc.). For CD4+ and CD8+ cells, the staining was performed as above. For Th1, Th2, and Th17 cells, we first stimulated at 37˚C for 4 h using a Stimulation Cocktail, then added 0.25 ul CD4 antibody and incubated at 4˚C for 0.5 h. The membrane was then broken according to the fixed membrane breaking kit instructions (cat. no. FMS-FP0100; fmacs Inc.). Finally, 0.625 μl of the corresponding IFN-γ, IL-4, and IL-17A antibodies were added and incubated at 4˚C for 0.5 h. For Treg cells, 0.25 μl of CD4 antibody was first added and 0.625 μl of CD25 antibody and incubated for 0.5 h 4˚C. Membrane rupture was then performed according to the instructions of the membrane rupture kit (eBioscience; Thermo Fisher Scientific, Inc.). Finally, Foxp3 antibody was added at 4˚C for 0.5 h. Tests were performed using a FACSCalibur system (BD Biosciences). Flow cytometry data were analyzed using the FlowJo software (V10.6; FlowJo LLC.).

Suppression assays. Spleens were gently ground into homogenate and filtered using 200 mesh filters to prepare MNCs. The MNCs were incubated in PBS, PH 7.2, containing 0.5% BSA and 2 mM EDTA. Isolation of $CD4^+CD25^+$ T cells was performed with microbeads magnetic separation provided by magnetic cell sorting (Miltenyi Biotec GmbH) from each group. $CD4^+CD25^-$ T cells (Teff) were collected from the control group. To investigate the suppression capacity, $CD4^+CD25^-$ T cells were first labelled with carboxyfluorescein diacetate succinimidyl ester (CFSE) dye (Invitrogen; Thermo Fisher Scientific, Inc.). Then $CFSE^+$ T cells were co-cultured with $CD4^+CD25^+$ T cells in RPMI 1640 containing 10% fetal bovine serum (Gibco; Thermo Fisher Scientific, Inc.) in a 1:1 or 2:1 ratio under the stimulation of IL-2 (1 $\mu g/10^6$ cells) and anti-CD3/CD28 antibody (1 $\mu g/10^6$ cells). The cells were cultured in 24-well plates for 72 h at 37˚C. $CFSE^+$ T cells were detected using FACS as described above.

Relative mRNA expressions detection. Shock-frozen lung tissue was homogenized in RNAiso Reagent (Takara Bio, Inc.). RNA was isolated using RNAiso Reagent (Takara Bio, Inc.) according to the manufacturer's instructions. Equal amounts of RNA were converted to cDNA using the Primerscript RT reagent kit (Takara Bio, Inc.) according to the manufacturer's protocol. Levels of mRNA were determined using Power SYBR Green PCR Master Mix (Applied Biosystems; Thermo Fisher Scientific, Inc.) with a StepOnePlus™ Real-Time PCR System (Applied Biosystems; Thermo Fisher Scientific, Inc.). The thermocycling conditions are listed in Table SII. Relative expression levels of mRNA were normalized to GAPDH. All of the values were expressed as $2^{-\Delta\Delta Cq}$ (21). Each sample was analyzed in triplicate. The primers pairs are listed in Table SI.

Statistical analysis. Data were analyzed using GraphPad Prism 8 (Dotmatics). Comparisons between cohorts were performed using an unpaired t-test. The t-test was used to calculate statistical differences between two populations. For multiple group comparisons, one-way ANOVA was used followed by Tukey's post-hoc analysis for group size ≥3. Data are expressed as the mean ± SEM (standard error of the mean). $P<0.05$ was considered to indicate a statistically significant difference.

Results

Establishment of experimental sarcoidosis with overactivated PI3K signaling. Histological examination confirmed the presence of a granulomatous group in the mouse model consisting of epithelioid cells and lymphocytes. This phenomenon is similar to granulomas in patients with sarcoidosis (Fig. 1B). Tested by FACS, the ratios of $CD4^+/CD8^+$ T cells in BALF in group sarcoidosis were increased significantly compared with the control group ($P=0.0012$). At the same time, no significant difference was observed in those in lymph nodes (Fig. 1C and D).

CAL-101/AS-605240 ameliorates pulmonary granuloma in sarcoidosis. Similar to those in group dexamethasone, granulomas in the lungs were significantly alleviated after treatment of CAL-101 (Fig. 2A). Notably, the alleviation of granulomas was more obvious in group CAL-101 compared with that in group AS-605240. To determine the mechanisms of these therapeutic effects of CAL-101/AS-605240, the balance of Th1/Th17/Tregs was then tested among groups at the selected time point (28 days following tail vein injection) when the number of Tregs was normal in disease phase. $CD4^+IFN\gamma^+$ T lymphocytes decreased after treatment of AS-605240 compared with the control, sarcoidosis, dexamethasone or CAL-101 groups ($P=0.001$, $P<0.0001$, $P=0.00125$ and $P=0.0003$, respectively) (AS-605240 vs. CAL-101) (Fig. 2B). Meanwhile, both $CD4^+IL\text{-}4^+$ and $CD4^+IL\text{-}17^+$ T lymphocytes showed no changes among groups (Fig. 2C and D). On day 53 after sensitization, when the number of Tregs showed no difference between group sarcoidosis and group normal, neither CAL-101 nor dexamethasone changed the Tregs ratio, whereas AS-605240 significantly decreased Tregs compared

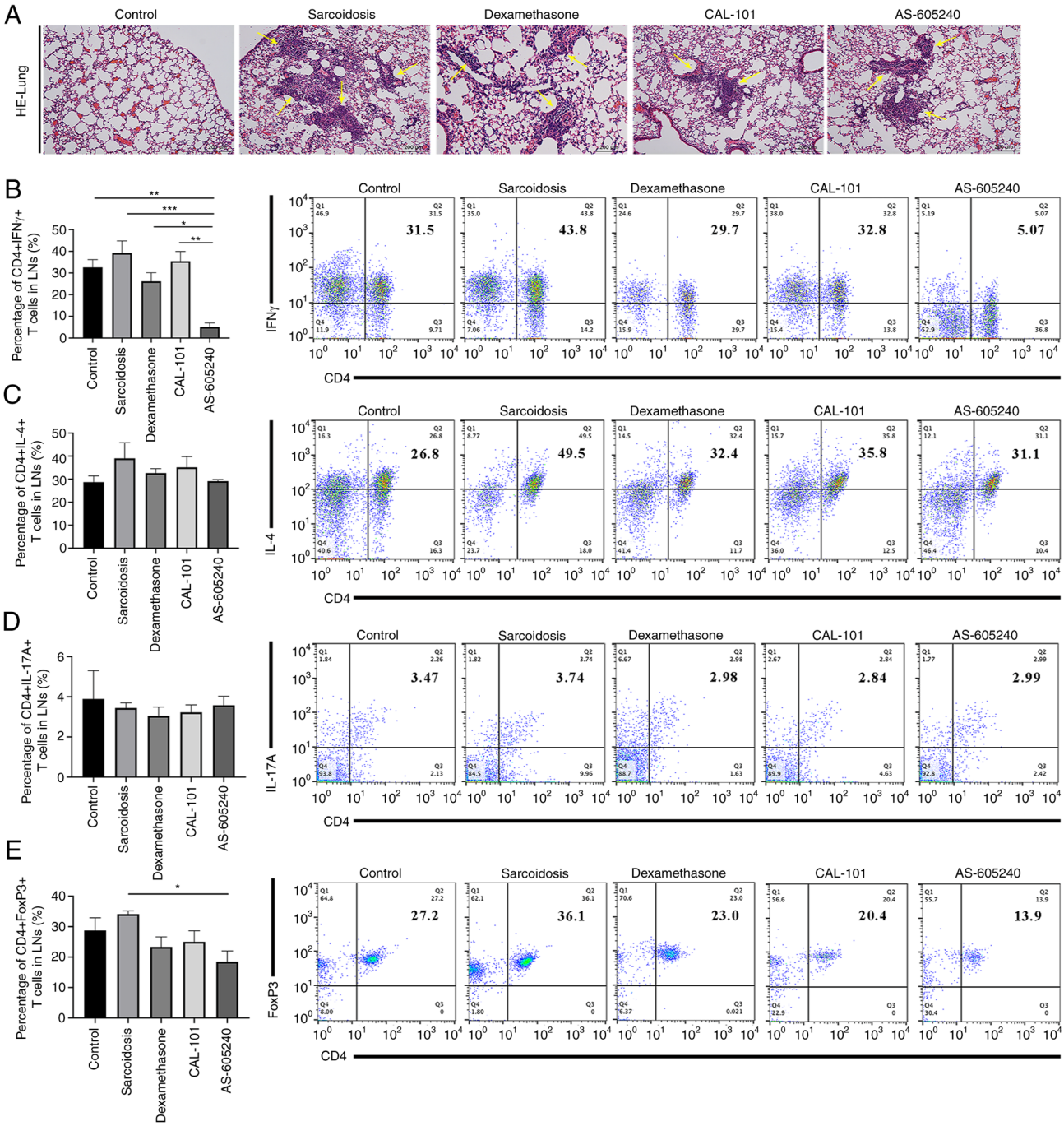

Figure 2. Histomorphology and cytological characteristics of SodA-induced sarcoidosis after treatments with CAL-101, AS-605240 or dexamethasone. (A) Histological images of lungs stained with hematoxylin and eosin. The yellow arrows indicate the pulmonary sarcoidosis granuloma. Magnification, x100. (B-E) The frequencies of (B) Th1, (C) Th2, (D) Th17 and (E) Tregs in lymph nodes from each group (n=6). *P<0.05, **P<0.01, ***P<0.0002. SodA, superoxidase A; IFNγ, interferon-gamma; IL-4, interleukin 4; IL-17, interleukin; FoxP3, forkhead box protein P3.

with those in the sarcoidosis group (P=0.0039; Fig. 2E). When examining Th1/Th2/Th17/Tregs related mRNA markers, CAL-101 was much more effective in normalizing relative expression levels of RORγt, FoxP3, IL-6 and IL-23 in sarcoidosis (P=0.0002, P=0.0293, P=0.0031 and P=0.0019, respectively) (Fig. 3C, D, F and G). Compared with AS-605240, CAL-101 was more effective in regulating the mRNA expression of Th1, Th2, Th17 and Treg (Fig. 3A, B, E and H). Collectively, AS-605240 showed obvious effects on decreasing Th1 and Tregs in SodA-induced sarcoidosis, suggesting the important role of PI3Kγ, rather than PI3Kδ, in modulating Th1 and Tregs differentiation in SodA-induced sarcoidosis.

PI3K inhibitors suppress activated PI3K/Akt signaling in both lungs and Tregs. The immunofluorescent assay demonstrated that there was increased p-PI3K and p-Akt expression in granulomas of the group sarcoidosis compared with control. Administration of CAL-101/AS-605240, as well as dexamethasone, significantly suppressed these activations, while CAL-101 showed a more profound effect compared with AS-605240 (Fig. 4A and B). Specifically, CAL-101

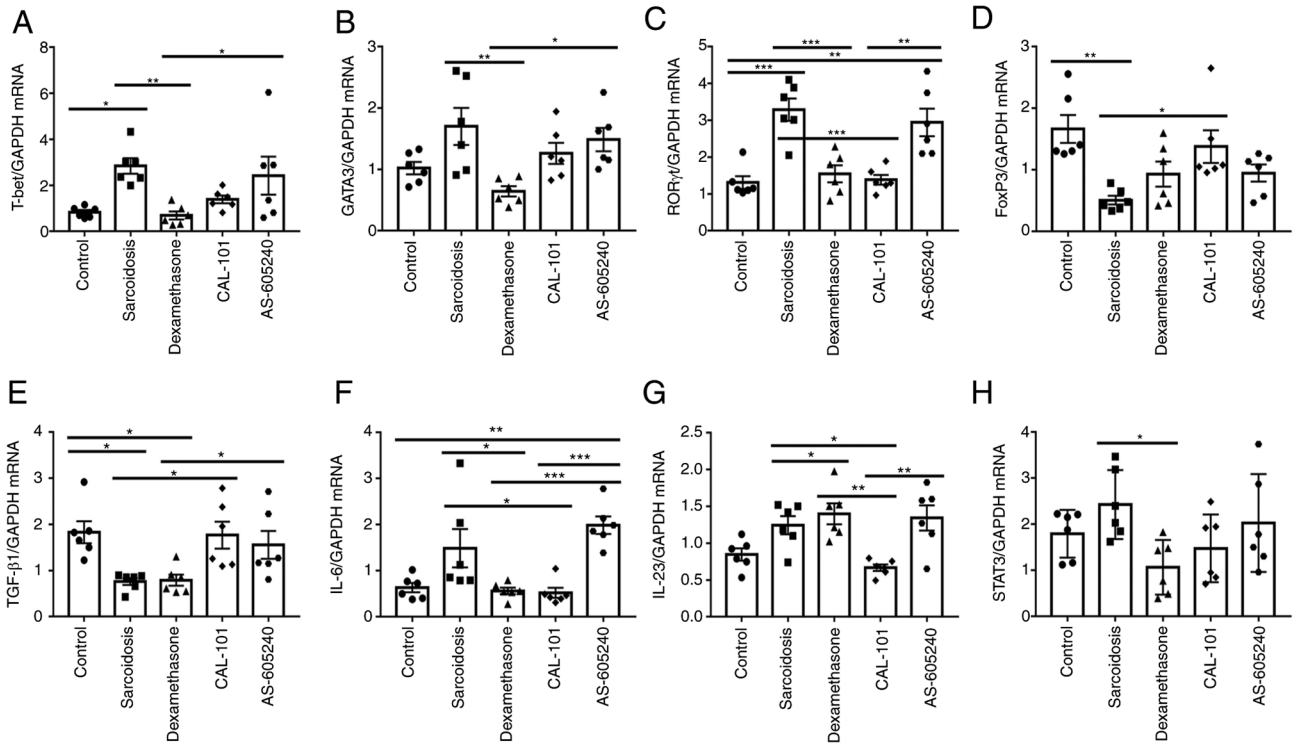

Figure 3. Th1, TH2, Th17 and Tregs-related mRNAs expression levels in each group. (A-H) reverse transcription-quantitative PCR was performed to determine relative expression levels of (A) *T-bet*, (B) *GATA3*, (C) *RORγt*, (D) *FoxP3*, (E) *TGF-β*, (F) *IL-6*, (G) *IL-23* and (H) *STAT3* (n=6). GAPDH served as internal control and three times repeats were performed. *P<0.05, **P<0.01, ***P<0.0002. FoxP3, forkhead box protein P3; IL, interleukin.

normalized p-PI3K and downregulated p-Akt (P<0.0001). By contrast, AS-605240 only downregulated p-PI3K but was less effective in suppressing p-Akt compared with CAL-101 (P<0.0001), suggesting the unique role of the PI3Kδ inhibitor in regulating PI3K/Akt signaling in the granuloma. On the other hand, $CD4^{+}CD25^{+}$ T cells also demonstrated high PI3K expression levels and Akt activity levels (P<0.0001). Upon CAL-101/AS-605240 treatment, the abnormal activation of PI3K/Akt signaling in $CD4^{+}CD25^{+}$ cells was also significantly recovered, with a stronger effect of CAL-101 compared with AS-605240 (P<0.05; Fig. 4C and D).

Inhibition of PI3K signaling rescues the suppressive function of Tregs in sarcoidosis. CAL-101 and AS-605240 inhibited the abnormal activation of PI3K/Akt signaling in Tregs, especially the former. To determine whether these inhibitions induced immune homeostasis in SodA-induced sarcoidosis, $CD4^{+}CD25^{+}$ cells (Tregs) were co-cultured with CFSE-labeled Teff in the presence of IL-2 and anti-CD3/CD28. As shown in Fig. 5, the proliferated $CFSE^{+}$ T cells were significantly increased in group sarcoidosis compared with the control group [P=0.0007 (1:1) and P=0.0131 (2:1), respectively], demonstrating an impaired suppressive function of Tregs in sarcoidosis. Similar to those in group dexamethasone, CAL-101 induced significant decreases of $CFSE^{+}$ T cells when $CD4^{+}CD25^{+}$ T cells were incubated with Teff at a ratio of 1:1 or 2:1 [P<0.0001 (1:1), and P=0.0004 (2:1), respectively] (Fig. 5A and B). Notably, AS-605240 was less effective than CAL-101 in inhibiting proliferation of CFSE+ T cells in sodium-induced sarcoidosis when CD4+CD25+ T cells were incubated in a 1:1 ratio with Teff cells (P=0.0003; Fig. 5A and C). Furthermore, AS-605240 still showed no effects on rescuing the function of Tregs when $CD4^{+}CD25^{+}$ T cells were incubated with Teff at a high ratio of 2:1 (Fig. 5B and D). By contrast, the effects of CAL-101 on suppressing $CFSE^{+}$ T cells proliferation were relatively steady.

Discussion

Altogether these results demonstrated that inhibition of PI3Kp110δ/p110γ by transtracheal CAL-101/AS-605240 administration ameliorated pulmonary granuloma in SodA-induced sarcoidosis. Therapeutic effects could be attributed to the inhibition of PI3K/Akt signaling both in granulomas and Tregs, particularly in rescuing Treg suppression. CAL-101 was more effective compared with AS-605240 in helping maintain the homeostasis of both Th1 and Tregs and in overcoming the aberrantly activated Akt in lungs and Tregs, which underlined that PI3Kδ played a more important role compared with PI3Kγ in immune modulation in SodA-induced sarcoidosis.

Class I PI3K is a heterodimeric enzyme consisting of a regulatory unit and a catalytic unit (p110α, p110β, p110γ or p110δ) (22,23). The expression of the p110δ and p110γ subunits is mainly restricted to leukocytes, whereas p110α and p110β are expressed by all cell types (9). Clinical trials with PI3K inhibitors in breast cancer, leukemia and lymphoma are showing encouraging results (24-27), highlighting the potential of PI3K inhibitors in cancer immunotherapy. PI3K/Akt signaling is usually dysregulated and increased, having multifaceted regulatory functions in the immune system, producing an autoimmune

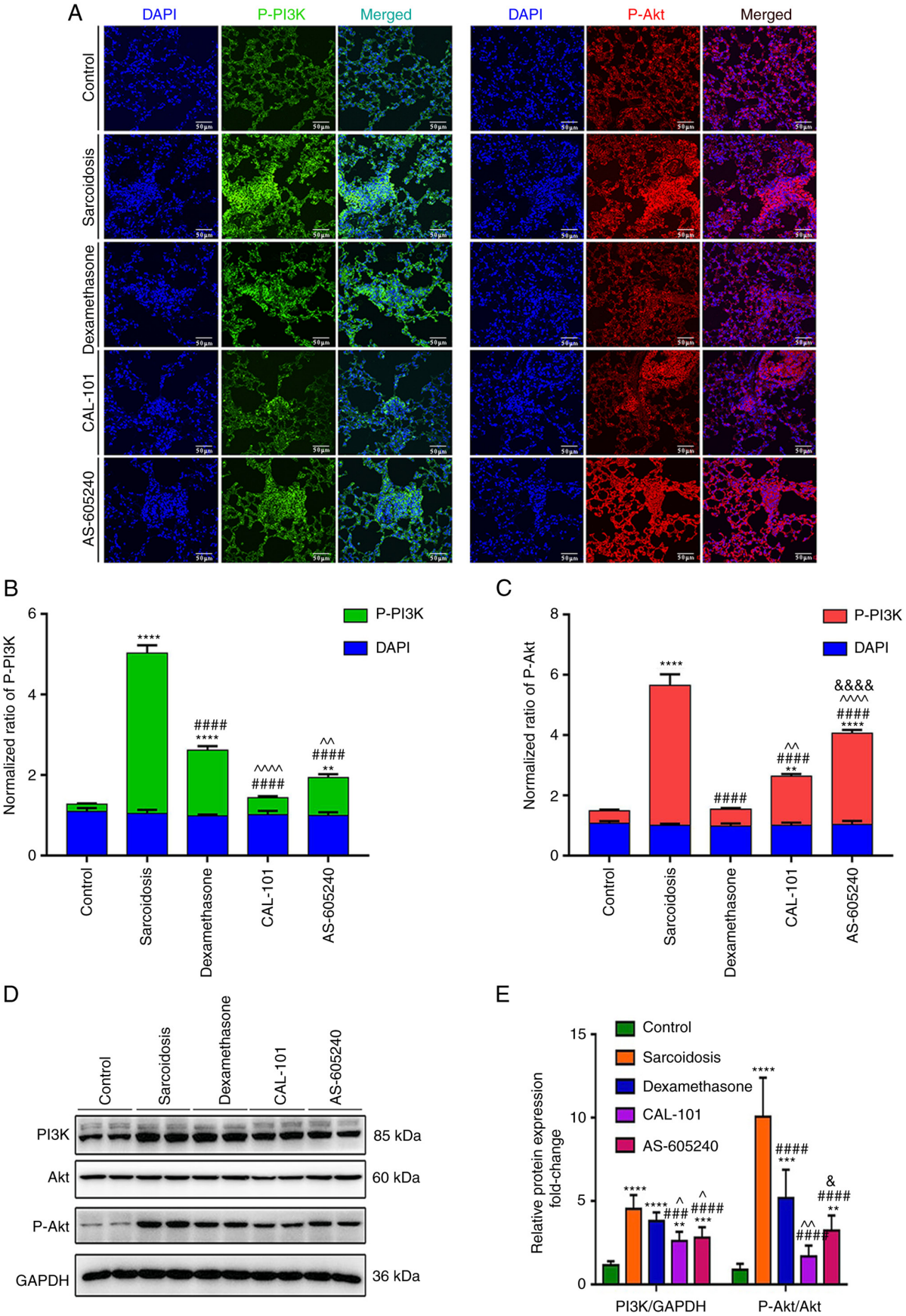

Figure 4. CAL-101/AS-605240 rescues the overactivation of the PI3K/AKT pathway in SodA-induced sarcoidosis. (A) Representative images showed the expression levels of p-PI3K (green) and p-AKT (red) in granulomas in each group. Magnification, x100. Summary of the mean fluorescence intensities of (B) p-PI3K, (C) p-AKT (top) and DAPI (bottom) in each group. (D) Western blot analysis (E) detecting expression levels of PI3K, p-PI3K, AKT and p-AKT in $CD4^+CD25^+$ T cells purified by MACS in each group. $^{**}P<0.01$, $^{***}P<0.002$, $^{****}P<0.0001$ vs. the control group; $^{\#\#\#}P<0.002$, $^{\#\#\#\#}P<0.0001$ vs. the sarcoidosis group; $^{\wedge}P<0.05$, $^{\wedge\wedge}P<0.01$, $^{\wedge\wedge\wedge\wedge}P<0.001$ compared with the dexamethasone group; $^{\&}P<0.05$, $^{\&\&\&\&}P<0.001$ vs. the CAL-101 group. SodA, superoxidase A; PI3K, Phosphoinositide 3-kinases; p-, phosphorylated-; MACS, magnetic cell sorting.

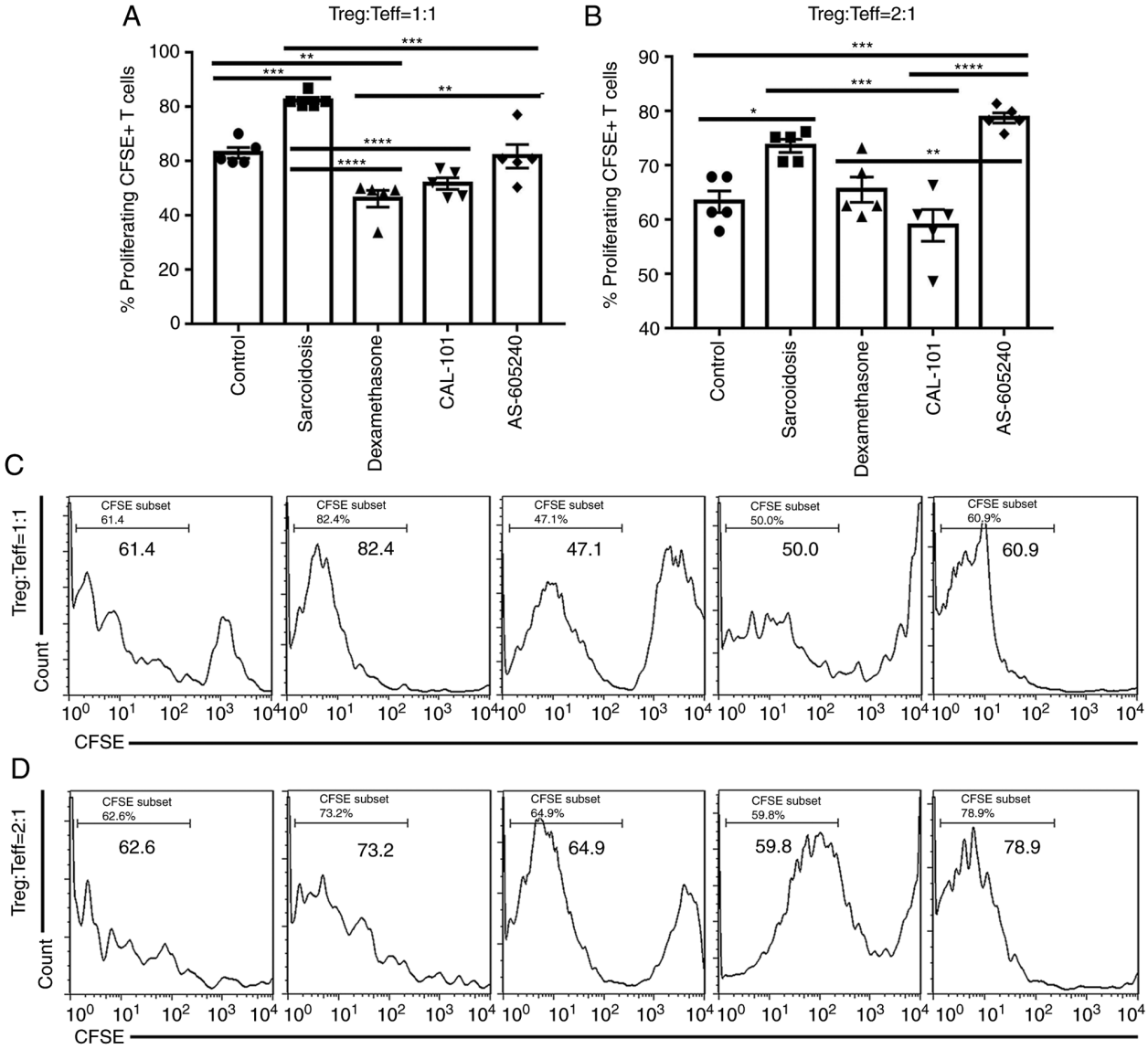

Figure 5. CAL-101/AS-605240 recovers the function of Tregs in SodA-induced sarcoidosis mice by regulating the PI3K pathway. $CD4^+CD25^+$ cells (Tregs) and $CD4^+CD25^-$ T cells (Teff) were separated from the spleen. $CD4^+CD25^+$ cells (Tregs) were co-cultured with $CD4^+CD25^-$ T cells (Teff) labeled with CFSE in the presence of IL-2 and anti-CD3/CD28 for 72 h. (A and B) The frequency of $CFSE^+$ T cells when Tregs and Teff were co-cultured at a ratio of (A) 1:1 and (B) 2:1 (n=6). (C and D) Representative histograms depicting proliferated $CFSE^+$ T cells when Treg and Teff were co-cultured at a ratio of (C) 1:1 and (D) 2:1. $^*P<0.05$, $^{**}P<0.01$, $^{***}P<0.0002$, $^{****}P<0.0001$. SodA, superoxidase A; CFSE, carboxyfluorescein diacetate succinimidyl ester.

phenotype in immune disorders (28,29). Aberrantly activated PI3K pathway leads to loss of tolerance, aberrant immune activation and production of autoantibody (19,30). Although p110γ and p110δ are preferentially expressed in immune cells, p110γ/p110δ inhibitors targeting these isoforms are reported to inhibit inflammatory activity in autoimmune and inflammatory diseases models by affecting the adaptive and innate immune response, such as collagen-induced arthritis, ovalbumin-induced asthma, microbiota-dependent colitis and systemic lupus erythematosus models (31,32), leading to potential therapeutic effects in multiple inflammatory and autoimmune diseases. Furthermore, clinical trials have also shown promising effects of PI3Kδ/γ inhibitors on immune disorders such as asthma, Sjögren's syndrome and allergic rhinitis (33-35), showing significant potential of PI3K inhibitors for clinical use.

Despite this, not all PI3K inhibitors can produce a good response in treatment. The effect of PI3K inhibitors targeting various subtypes differ in different autoimmune diseases. To the best of our knowledge, there are few studies on the use of PI3K inhibitors in the treatment of sarcoidosis. In the treatment of other autoimmune diseases, it has been revealed that not all PI3Kγ/δ inhibitors can produce a good response in treatment (36-38). In the experimental autoimmune encephalomyelitis (EAE) mouse model, the PI3Kδ-selective inhibitor does not affect the progression of T cell-mediated autoimmune inflammation or disease severity (36). By contrast, PI3Kγ inhibitor significantly alleviates the severity of EAE, and significantly reduces leukocyte infiltration in the central nervous system (37). For the experimental epidermolysis bullosa acquisita, a PI3Kβ-selective inhibitor is more effective compared with a PI3Kδ-selective one in inhibiting neutrophil-driven inflammation (38). Whether other selective

PI3Kγ/δ inhibitors have the same therapeutic effect remains to be verified, and further experiments will be conducted in the future. Thus, discussing the most effective PI3K subtypes in treating sarcoidosis is reasonable.

In sarcoidosis, PI3K signaling is one of the most aberrantly activated pathways. Our early study demonstrated that inhibition of PI3K/Akt signaling by BKM120 or LY294002 can ameliorate granuloma (14,17). Previous results implied that co-inhibiting the PI3Kγ subunit is more efficient in augmenting therapies when using non-selective PI3K inhibitors (17). The current study aimed to determine the selective PI3K inhibitors that would optimize therapy. Although the distinction is not absolute, PI3Kγ is functionally dominant in myeloid cells (19). It plays a key role in chemokine-mediated recruitment and activation of innate immune cells at sites of inflammation, whereas PI3Kδ is highly expressed in leukocytes and is crucial in antigen receptor and cytokine-mediated B and T cell development, differentiation and function (39). They may be capable of modulating the Th1/Tregs/Th17 paradigm due to their diverse roles in diverse immune functions. In that case, the present study tested whether the presence of PI3Kδ or PI3Kγ inhibition by CAL-101 or AS-605240 would benefit SodA-induced sarcoidosis on the selected time point when the number of Tregs was normal. The results turned out to be more complex than anticipated. When PI3Kδ inhibitor induced more profound therapeutic effects compared with the PI3Kγ inhibitor, PI3Kδ and PI3Kγ may work together to generate a functional output in SodA-induced sarcoidosis.

Overall, studies suggest that sarcoidosis is considered a model of persistent inflammation caused by abnormalities in Th1/Th2 and Treg/Th17 paradigms and impaired the function of Tregs (7,8). The homeostatic ratio of circulating Tregs/Th17 inversely trends with sarcoidosis activity, decreasing in the relapsed patients and increasing back to normal ranges in non-active sarcoidosis or with treatment with corticosteroids (15,40). In addition, the increase in the function of Tregs is associated with improvements in clinical measures of sarcoidosis (1,11). In our previous study, inhibition of PI3Ks by BKM120 or LY294002 was show to significantly improve pulmonary granuloma, ameliorate both Th1/Th2 and Tregs/Th17 disorders and restore the suppressive function of Tregs in SodA-induced sarcoidosis at the time point when there was a Tregs/Th17 imbalance (17). Furthermore, the present study showed the effects of CAL-101 and AS-605240 on rescuing the suppressive functions of Tregs at the selected time point with normal Tregs ratios. However, notably, AS-605240 adversely affected the balance between Th1 and Treg in a less potent manner compared with CAL-101. These findings are in line with the key role of the Th1/Tregs/Th17 paradigm in the pathogenesis of sarcoidosis (7,8,15,40), though the question of how PI3K inhibitors slow the development of granuloma in this setting remains unsolved.

Mechanistic studies highlight the potential importance of the PI3K/Akt signaling on the activation, differentiation and function of both Tregs and T effector cells, while PI3K signaling has been identified as a nodal control point for Tregs homeostasis and stability (18,41,42). Tregs seem to respond more easily to cancer immunotherapy compared with other T cell populations, even though the mechanism of action is still unclear (43,44). Inhibition of PI3Kγ and PI3Kδ both restrict the expansion of alloreactive T cells in a mouse allograft transplantation model. However, PI3Kδ inhibition instead of concurrent p110γ deficiency detrimentally affects the function of Tregs (41). In addition, PI3Kγ inhibition may compensate for the negative effect of PI3Kδ inhibition on long-term allograft survival (41). PI3Kγ and PI3Kδ inhibition may synergistically modulate immune responses. While selective inhibition of only PI3Kδ is weakly anti-inflammatory, dual inhibition of PI3Kγ and δ has superior anti-inflammatory effects (45,46). Moreover, PI3Kδ/γ inhibition yields an anti-inflammatory signature distinct from pan-PI3K inhibition and known anti-inflammatory drugs (46). Consistent with the findings of these reports, the present study demonstrated that PI3Kδ inhibition could overcome the aberrantly activated Akt in the lungs and Tregs, thus maintaining the function of Tregs. By contrast, PI3Kγ inhibition was less effective in recovering PI3K/Akt signaling in granuloma and Tregs but even dampened Th1/Tregs balance. Considering that BKM120 was previously found to have a more profound effect on granuloma improvement compared with LY294002 (17), synergistic effects of PI3Kγ and PI3Kδ may occur in immune modulation in SodA-induced sarcoidosis.

In conclusion, these results indicated that pharmacological inhibition of PI3Kδ by CAL-101 may be an effective immunoregulatory strategy in treating diseases with deficient suppressive functions of Tregs, such as sarcoidosis. Moreover, it appears that inhibition of PI3Kδ is more efficient compared with PI3Kγ, despite the possibility that synergism of these two PI3K subunits may occur. Although it remains unknown whether dual inhibition of PI3Kγ and PI3Kδ has an improved effect on immune modulation under the distinct pathophysiological processes, PI3Kγ/δ inhibitors may be developed into a new therapeutic principle for sarcoidosis.

Acknowledgements

Not applicable.

Funding

This work was supported by the National Natural Science Foundation of China (grant nos. 81100386 and 81400046) and the Independent and Open Grant of Jiangsu Key Laboratory of Molecular Medicine and Innovation and Entrepreneurship Training Program for College Students (grant nos. G201910284011 and 202010284016Z).

Availability of data and materials

The datasets used and/or analyzed during the current study are available from the corresponding author on reasonable request.

Authors' contributions

XZ participated in data interpretation and wrote the manuscript. QD performed the experiments and analyzed the data. JS, SZ, BZ, SL, YZ, YiW, XL, XJ and DL collected and assembled data. JD analyzed the data and improved the language of the manuscript. YaW contributed to the design of the study,

received funding and supervised the study. YoW reviewed and edited the manuscript and provided administrative support for the study. QD and XZ confirm the authenticity of all the raw data. All authors read and approved the final manuscript.

Ethics approval and consent to participate

All experimental protocols were approved under a project license (approval no. SCXK-Jiangsu-2019-0056) granted by the Institutional Animal Care and Use Committee of Nanjing University, in compliance with institutional guidelines for the care and use of animals.

Patient consent for publication

Not applicable.

Competing interests

The authors declare that they have no competing interests.

References

1. Broos CE, van Nimwegen M, Hoogsteden HC, Hendriks RW, Kool M and van den Blink B: Granuloma formation in pulmonary sarcoidosis. Front Immunol 4: 437, 2013.
2. Hunninghake GW, Costabel U, Ando M, Baughman R, Cordier JF, du Bois R, Eklund A, Kitaichi M, Lynch J, Rizzato G, *et al*: ATS/ERS/WASOG statement on sarcoidosis. American thoracic society/european respiratory society/world association of sarcoidosis and other granulomatous disorders. Sarcoidosis Vasc Diffuse Lung Dis 16: 149-173, 1999.
3. Oswald-Richter KA, Richmond BW, Braun NA, Isom J, Abraham S, Taylor TR, Drake JM, Culver DA, Wilkes DS and Drake WP: Reversal of global CD4+ subset dysfunction is associated with spontaneous clinical resolution of pulmonary sarcoidosis. J Immunol 190: 5446-5453, 2013.
4. Cinetto F and Agostini C: Advances in understanding the immunopathology of sarcoidosis and implications on therapy. Expert Rev Clin Immunol 12: 973-988, 2016.
5. Iannuzzi MC, Rybicki BA and Teirstein AS: Sarcoidosis. N Engl J Med 357: 2153-2165, 2007.
6. Gurram RK, Kujur W, Maurya SK and Agrewala JN: Caerulomycin A enhances transforming growth factor-β (TGF-β)-Smad3 protein signaling by suppressing interferon-γ (IFN-γ)-signal transducer and activator of transcription 1 (STAT1) protein signaling to expand regulatory T cells (Tregs). J Biol Chem 289: 17515-17528, 2014.
7. Ten Berge B, Klein Jan A, Muskens F, Hammad H, Hoogsteden HC, Hendriks RW, Lambrecht BN and Van den Blink B: Evidence for local dendritic cell activation in pulmonary sarcoidosis. Respir Res 13: 33, 2012.
8. Patterson KC and Chen ES: The pathogenesis of pulmonary sarcoidosis and implications for treatment. Chest 153: 1432-1442, 2018.
9. Miyara M, Amoura Z, Parizot C, Badoual C, Dorgham K, Trad S, Kambouchner M, Valeyre D, Chapelon-Abric C, Debré P, *et al*: The immune paradox of sarcoidosis and regulatory T cells. J Exp Med 203: 359-370, 2006.
10. Idali F, Wahlström J, Müller-Suur C, Eklund A and Grunewald J: Analysis of regulatory T cell associated forkhead box P3 expression in the lungs of patients with sarcoidosis. Clin Exp Immunol 152: 127-137, 2008.
11. Prasse A, Zissel G, Lützen N, Schupp J, Schmiedlin R, Gonzalez-Rey E, Rensing-Ehl A, Bacher G, Cavalli V, Bevec D, *et al*: Inhaled vasoactive intestinal peptide exerts immunoregulatory effects in sarcoidosis. Am J Respir Crit Care Med 182: 540-548, 2010.
12. Taflin C, Miyara M, Nochy D, Valeyre D, Naccache JM, Altare F, Salek-Peyron P, Badoual C, Bruneval P, Haroche J, *et al*: FoxP3+ regulatory T cells suppress early stages of granuloma formation but have little impact on sarcoidosis lesions. Am J Pathol 174: 497-508, 2009.
13. Rappl G, Pabst S, Riemann D, Schmidt A, Wickenhauser C, Schütte W, Hombach AA, Seliger B, Grohé C and Abken H: Regulatory T cells with reduced repressor capacities are extensively amplified in pulmonary sarcoid lesions and sustain granuloma formation. Clin Immunol 140: 71-83, 2011.
14. Ding J, Dai J, Cai H, Gao Q and Wen Y: Extensively disturbance of regulatory T cells-Th17 cells balance in stage II pulmonary sarcoidosis. Int J Med Sci 14: 1136-1142, 2017.
15. Zissel G and Müller-Quernheim J: Cellular players in the immunopathogenesis of sarcoidosis. Clin Chest Med 36: 549-560, 2015.
16. Zhang B, Zhao F, Mao H, Ma W, Zhang Y, Zhang X, Ding J, Gao Q and Wen Y: Interleukin 33 ameliorates disturbance of regulatory T cells in pulmonary sarcoidosis. Int Immunopharmacol 64: 208-216, 2018.
17. Zhang B, Dai Q, Jin X, Liang D, Li X, Lu H, Liu Y, Ding J, Gao Q and Wen Y: Phosphoinositide 3-kinase/protein kinase B inhibition restores regulatory T cell's function in pulmonary sarcoidosis. J Cell Physiol 234: 19911-19920, 2019.
18. Huynh A, DuPage M, Priyadharshini B, Sage PT, Quiros J, Borges CM, Townamchai N, Gerriets VA, Rathmell JC, Sharpe AH, *et al*: Control of PI(3) kinase in Treg cells maintains homeostasis and lineage stability. Nat Immunol 16: 188-196, 2015.
19. Greaves SA, Peterson JN, Strauch P, Torres RM and Pelanda R: Active PI3K abrogates central tolerance in high-avidity autoreactive B cells. J Exp Med 216: 1135-1153, 2019.
20. Swaisgood CM, Oswald-Richter K, Moeller SD, Klemenc JM, Ruple LM, Farver CF, Drake JM, Culver DA and Drake WP: Development of a sarcoidosis murine lung granuloma model using mycobacterium superoxide dismutase A peptide. Am J Respir Cell Mol Biol 44: 166-174, 2011.
21. Livak KJ and Schmittgen TD: Analysis of relative gene expression data using real-time quantitative PCR and the 2(-Delta Delta C(T)) method. Methods 25: 402-408, 2001.
22. Abdel-Magid AF: Potential of PI3Kβ inhibitors in the treatment of cancer and other diseases. ACS Med Chem Lett 8: 778-780, 2017.
23. Rathinaswamy MK and Burke JE: Class I phosphoinositide 3-kinase (PI3K) regulatory subunits and their roles in signaling and disease. Adv Biol Regul 75: 100657, 2020.
24. Scott WJ, Hentemann MF, Rowley RB, Bull CO, Jenkins S, Bullion AM, Johnson J, Redman A, Robbins AH, Esler W, *et al*: Discovery and SAR of novel 2,3-dihydroimidazo[1,2-c] quinazoline PI3K inhibitors: Identification of copanlisib (BAY 80-6946). ChemMedChem 11: 1517-1530, 2016.
25. Lannutti BJ, Meadows SA, Herman SE, Kashishian A, Steiner B, Johnson AJ, Byrd JC, Tyner JW, Loriaux MM, Deininger M, *et al*: CAL-101, a p110delta selective phosphatidylinositol-3-kinase inhibitor for the treatment of B-cell malignancies, inhibits PI3K signaling and cellular viability. Blood 117: 591-594, 2011.
26. Furet P, Guagnano V, Fairhurst RA, Imbach-Weese P, Bruce I, Knapp M, Fritsch C, Blasco F, Blanz J, Aichholz R, *et al*: Discovery of NVP-BYL719 a potent and selective phosphatidylinositol-3 kinase alpha inhibitor selected for clinical evaluation. Bioorg Med Chem Lett 23: 3741-3748, 2013.
27. Burris HA III, Flinn IW, Patel MR, Fenske TS, Deng C, Brander DM, Gutierrez M, Essell JH, Kuhn JG, Miskin HP, *et al*: Umbralisib, a novel PI3Kδ and casein kinase-1ε inhibitor, in relapsed or refractory chronic lymphocytic leukaemia and lymphoma: An open-label, phase 1, dose-escalation, first-in-human study. Lancet Oncol 19: 486-496, 2018.
28. Patel RK and Mohan C: PI3K/AKT signaling and systemic autoimmunity. Immunol Res 31: 47-55, 2005.
29. Adefemi F, Fruman DA and Marshall AJ: A case for phosphoinositide 3-kinase-targeted therapy for infectious disease. J Immunol 205: 3237-3245, 2020.
30. Franks SE, Getahun A and Cambier JC: A precision B cell-targeted therapeutic approach to autoimmunity caused by phosphatidylinositol 3-kinase pathway dysregulation. J Immunol 202: 3381-3393, 2019.
31. Winkler DG, Faia KL, DiNitto JP, Ali JA, White KF, Brophy EE, Pink MM, Proctor JL, Lussier J, Martin CM, *et al*: PI3K-δ and PI3K-γ inhibition by IPI-145 abrogates immune responses and suppresses activity in autoimmune and inflammatory disease models. Chem Biol 20: 1364-1374, 2013.
32. Steinbach EC, Kobayashi T, Russo SM, Sheikh SZ, Gipson GR, Kennedy ST, Uno JK, Mishima Y, Borst LB, Liu B, *et al*: Innate PI3K p110δ regulates Th1/Th17 development and microbiota-dependent colitis. J Immunol 192: 3958-3968, 2014.

33. Juarez M, Diaz N, Johnston GI, Nayar S, Payne A, Helmer E, Cain D, Williams P, Devauchelle-Pensec V, Fisher BA, *et al*: A phase 2 randomized, double-blind, placebo-controlled, proof-of-concept study of oral seletalisib in primary Sjögren's syndrome. Rheumatology (Oxford) 60: 1364-1375, 2021.
34. Horak F, Puri KD, Steiner BH, Holes L, Xing G, Zieglmayer P, Zieglmayer R, Lemell P and Yu A: Randomized phase 1 study of the phosphatidylinositol 3-kinase δ inhibitor idelalisib in patients with allergic rhinitis. J Allergy Clin Immunol 137: 1733-1741, 2016.
35. Perry MWD, Bjorhall K, Bold P, Brűlls M, Börjesson U, Carlsson J, Chang HA, Chen Y, Eriksson A, Fihn BM, *et al*: Discovery of AZD8154, a dual PI3Kγδ inhibitor for the treatment of asthma. J Med Chem 64: 8053-8075, 2021.
36. Stark AK, Davenport ECM, Patton DT, Scudamore CL, Vanhaesebroeck B, Veldhoen M, Garden OA and Okkenhaug K: Loss of phosphatidylinositol 3-kinase activity in regulatory T cells leads to neuronal inflammation. J Immunol 205: 78-89, 2020.
37. Li H, Park D, Abdul-Muneer PM, Xu B, Wang H, Xing B, Wu D and Li S: PI3Kγ inhibition alleviates symptoms and increases axon number in experimental autoimmune encephalomyelitis mice. Neuroscience 253: 89-99, 2013.
38. Zillikens H, Kasprick A, Osterloh C, Gross N, Radziewitz M, Hass C, Hartmann V, Behnen-Härer M, Ernst N, Boch K, *et al*: Topical application of the PI3Kβ-selective small molecule inhibitor TGX-221 Is an effective treatment option for experimental epidermolysis bullosa acquisita. Front Med (Lausanne) 8: 713312, 2021.
39. Hawkins PT and Stephens LR: PI3K signalling in inflammation. Biochim Biophys Acta 1851: 882-897, 2015.
40. Liu Y, Qiu L, Wang Y, Aimurola H, Zhao Y, Li S and Xu Z: The circulating Treg/Th17 cell ratio is correlated with relapse and treatment response in pulmonary sarcoidosis patients after corticosteroid withdrawal. PLoS One 11: e0148207, 2016.
41. Uehara M, McGrath MM, Ohori S, Solhjou Z, Banouni N, Routray S, Evans C, DiNitto JP, Elkhal A, Turka LA, *et al*: Regulation of T cell alloimmunity by PI3Kγ and PI3Kδ. Nat Commun 8: 951, 2017.
42. Gamper CJ and Powell JD: All PI3Kinase signaling is not mTOR: Dissecting mTOR-dependent and independent signaling pathways in T cells. Front Immunol 3: 312, 2012.
43. Lim EL and Okkenhaug K: Phosphoinositide 3-kinase δ is a regulatory T-cell target in cancer immunotherapy. Immunology 157: 210-218, 2019.
44. Vanhaesebroeck B, Perry MWD, Brown JR, André F and Okkenhaug K: PI3K inhibitors are finally coming of age. Nat Rev Drug Discov 20: 741-769, 2021.
45. Randis TM, Puri KD, Zhou H and Diacovo TG: Role of PI3Kdelta and PI3Kgamma in inflammatory arthritis and tissue localization of neutrophils. Eur J Immunol 38: 1215-1224, 2008.
46. Williams O, Houseman BT, Kunkel EJ, Aizenstein B, Hoffman R, Knight ZA and Shokat KM: Discovery of dual inhibitors of the immune cell PI3Ks p110delta and p110gamma: A prototype for new anti-inflammatory drugs. Chem Biol 17: 123-134, 2010.